ELSEVIER

1 August 1999

Optics Communications 166 (1999) 163–171

OPTICS COMMUNICATIONS

www.elsevier.com/locate/optcom

Full length article

Optical evaluation of fractality of rough surfaces using fractal illumination

Naoya Wada [a], Jun Uozumi [b,*], Toshimitsu Asakura [c]

[a] *Communications Research Laboratory, M.P.T., 4-2-1, Nukuikita, Koganei, Tokyo 184-8795, Japan*
[b] *Research Institute for Electronic Science, Hokkaido University, Sapporo, Hokkaido 060-0812, Japan*
[c] *Faculty of Engineering, Hokkai-Gakuen University, Sapporo, Hokkaido 064-0926, Japan*

Received 15 February 1999; accepted 10 May 1999

Abstract

A novel fractal illumination method is introduced to analyze the fractality of rough surfaces. In computer simulations, some different self-affine random surfaces are employed as models of rough surfaces having the fractality, and their scaling factors are evaluated by the proposed method. The results are compared with those obtained by an array illumination method. The sensitivity of these methods toward the scaling factor is discussed. The method is applied to three different actual rough surfaces, and their fractalities are evaluated experimentally. The effectiveness of the proposed method is shown.

PACS: 42.30.Va; 06.30.Bp; 47.53.+n
Keywords: Fractal rough surface; Self-affine surface; Scaling factor; Power spectrum; Cantor illumination

1. Introduction

To characterize rough surfaces, RMS (root-mean-square)-roughness has been used most frequently. In recent years, however, it has become clear that a certain class of actual surfaces has complicated structures with scale-invariant features and is not effectively characterized only by the RMS-roughness since such structures do not have characteristic lengths [1]. The scale-invariant feature of rough surfaces has attracted great interest in many fields [2–6] and is called fractality. The surface with this feature is a fractal surface. To evaluate the fractality of the surfaces in a noncontact and nondestructive way, some optical methods analyzing the fields diffracted or scattered coherently by surfaces are investigated [7–15]. However, these methods have some problems to be mentioned in the following. The power law representing the fractality of objects may not certainly appear in the diffracted or scattered field if the object is a surface fractal [1]. Even if the power law appears in the field, it is not practically easy to detect precisely the power law because the strong low and the weak high spatial frequency components coexisting in the field require

* Corresponding author. Present address: Faculty of Engineering, Hokkai-Gakuen University, Sapporo, Hokkaido 064-0926, Japan; e-mail: uozomi@eli.hokkai-s-u.ac.jp

0030-4018/99/$ - see front matter
PII: S0030-4018(99)00249-7

a detector with a very wide dynamic range. Furthermore, if the surface has several different kinds of fractality within an illuminated area, it is almost impossible to detect each fractality separately.

To overcome these problems, we have introduced an optical method using an array illumination and applied it to some fractal surfaces [16]. The effectiveness of this method was investigated by means of computer simulations and experiments. In the study, it was elucidated that the vertical and horizontal scaling factors, which characterize the fractality of the surface, can be determined by two quantities being measurable in experiments. However, a sensitivity of this method is not sufficiently high and not stationary.

In this paper, to evaluate more precisely the scaling property of surfaces, a method using a fractal illumination is introduced and is applied to the fractal surfaces employed in Ref. [16]. The effectiveness of this novel method is investigated by means of computer simulations and experiments. The results are compared with those obtained by the array illumination method.

2. Principle

The principle of a fractal illumination method is basically similar with the array illumination method [16]. The fractal surface is illuminated by the incident light having a grating-like intensity distribution with an incident angle θ_1 as shown in Fig. 1(a). Then, a regular grating pattern G_1 is formed on the surface. If we observe an image of this pattern formed in another direction with an angle θ_2, the imaged pattern G_2 is no longer regular because the image of each element of the regular pattern is shifted according to an irregularity of the surface. If the surface is flat, the regular grating pattern of the incident light impinges on the positions indicated by gray dots in Fig. 1(b) and, hence, the observed pattern is also a regular grating. However, in case of the rough surface, the grating pattern of the incident light impinges on the positions indicated by black dots in Fig. 1(b) and, hence, the elements of the observed grating pattern are shifted by lengths e_1, e_2, e_3, and so on, which depend upon heights of the

Fig. 1. Schematic representation of (a) the measuring system and (b) the modulation mechanism of the grating pattern by the surface.

imaging points. A relation between the surface height h above the mean surface at each array element of the incident light and the corresponding shift e is given by

$$e = \frac{\sin(\theta_1 + \theta_2)}{\cos\theta_1} h. \quad (1)$$

Namely, the regular grating pattern G_1 is modulated by the random height of the fractal surface and becomes a randomized grating pattern G_2 involving a scaling fluctuation. The information about the fractality of the surface is extracted by analyzing this randomized grating pattern [17].

In the array illumination case, it has been found that the ensemble-averaged power spectra of the randomized grating pattern have periodic major max-

ima with an increase of the spatial frequency and that the values of the major maxima decrease with the power law. From this power law, we can determine the ratio of two important vertical and horizontal scaling parameters; which characterize the scaling property of fractal surfaces. For more detailed results refer to Ref. [16].

In this paper, we use a fractal illumination which has an intensity distribution having a form of the triadic Cantor grating of level 6 [2], instead of the array illumination. The conventional array illumination pattern used in Ref. [16] and the proporsed Cantor illumination are schematically represented in Fig. 2. The Cantor grating is considered to be a multiscale grating. In Fig. 2, the Cantor illumination pattern is given by product of the different scale periodic grating patterns. The Cantor grating is also modulated by the fractal surface in the same way with the array illumination case and becomes a randomized Cantor grating pattern which involves the scaling fluctuation reflecting the fractality of the surface. Hence, the scaling property of the surface can be revealed by analyzing the randomized Cantor grating pattern.

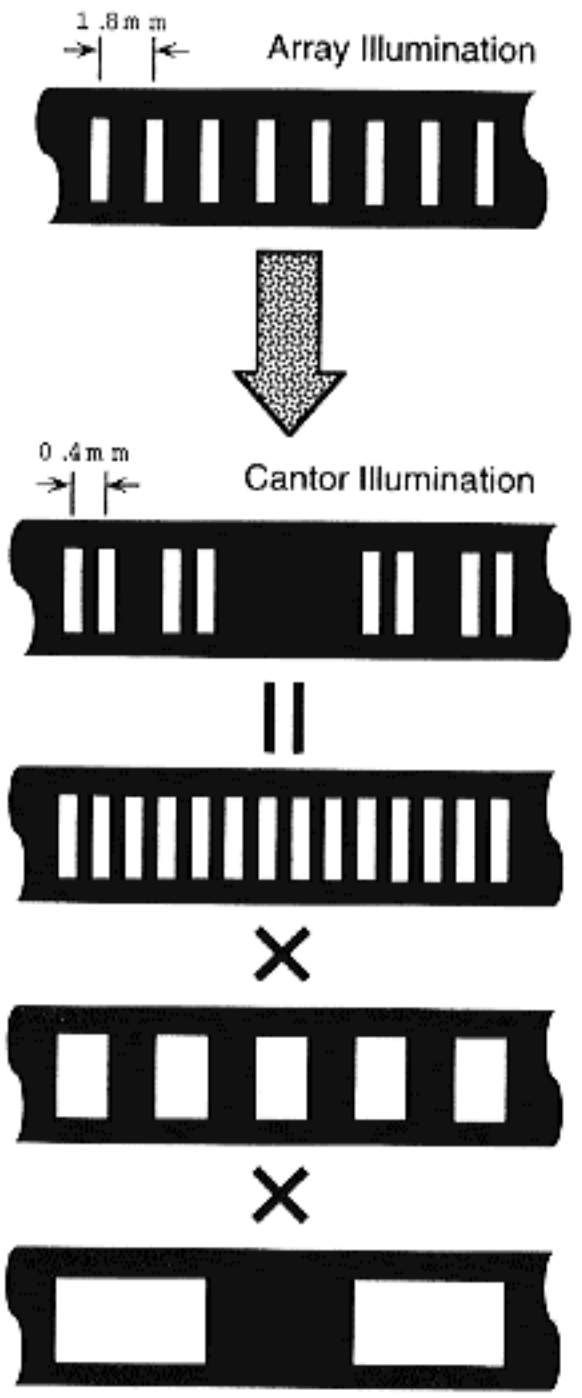

Fig. 2. A portion of the array illumination pattern (top) and the Cantor illumination pattern (bottom).

3. Simulation

3.1. Surface model

The optical system and the surface model assumed in present simulations are similar with those used in simulations of the array illumination method [16], apart from the pattern of incident light. The self-affine surfaces are employed as a typical model of fractal surfaces. The height $h(x)$ of the surface is represented by

$$h(x) = A \sum_{i=1}^{N} \gamma_v^{1-i} a_i(x), \tag{2}$$

where N is a number of superpositions and is called a level, γ_v is a vertical scaling factor governing the vertical scaling property of the surface, and $a_i(x)$ stands for the random process whose amplitude distribution obeys a zero-mean Gaussian probability density function with a certain standard deviation σ_a. $a_i(x)$ is constant within an interval given by

$$l_i = \alpha \gamma_h^{1-i} \tag{3}$$

and is independent of its value in a different interval. In Eq. (3), γ_h is a factor governing the horizontal scaling property and is called a horizontal scaling factor (see Appendix A). In addition, the incident angle is assumed to take $\theta_i = 0$. This means that the surface is illuminated normally to reduce the effect of shadowing on the surface.

3.2. Fractal illumination model

The fractal illumination with the Cantor grating pattern of level 6, $C_6(x)$, is expressed by

$$\begin{aligned} C_6(x) &= [\delta(x+L/3)+\delta(x-L/3)] \\ &\otimes[\delta(x+L/3^2)+\delta(x-L/3^2)] \\ &\vdots \\ &\otimes[\delta(x+L/3^6)+\delta(x-L/3^6)] \\ &\otimes E_6(x), \end{aligned}$$

where $\delta(x)$ is the Dirac delta function and $\otimes$ stands for the convolution operation. In Eq. (4), $E_6(x)$ represents a shape of the segment of level 6 which is expressed by

$$E_6(x) = \begin{cases} A & |x| \le L/(2\cdot 3^6) \\ 0 & |x| > L/(2\cdot 3^6) \end{cases}$$
$$= A\,\mathrm{rect}(2\cdot 3^6 x/L), \qquad (4)$$

where A is an intensity of the incident light. The pattern represented in Fig. 2 is a portion of this Cantor illumination model.

3.3. Calculation and results

On the basis of the simulation model, 200 data of the Cantor grating patterns modulated randomly by the fractal surface are calculated for each of several surfaces with different values of vertical scaling factor γ_v, horizontal scaling factor γ_h, standard deviation σ_f of fluctuations on the surface, level N of the scaling property, and detecting angle θ_2. Subsequently, the ensemble average $\mathrm{E}\{S'(u)\}$ of the modified power spectra $S'(u) = P(u)/F(u)$ of the modulated Cantor grating patterns is calculated, and several results normalized by the central peak value $S(0)$ of a modified power spectrum for the Cantor grating pattern without fluctuations are shown in Fig. 3(a)–(d) as a function of the spatial frequency u for $(u_0, 3^6u_0)$ in a log-log representation. Here, $P(u)$ stands for the power spectrum of the modulated Cantor grating pattern, $F(u)$ is the Fourier transform of the shape of an element given by Eq. (4), and u_0 is the spatial frequency given by

$$u_0 = \frac{3}{4L\cos\theta_2}, \qquad (5)$$

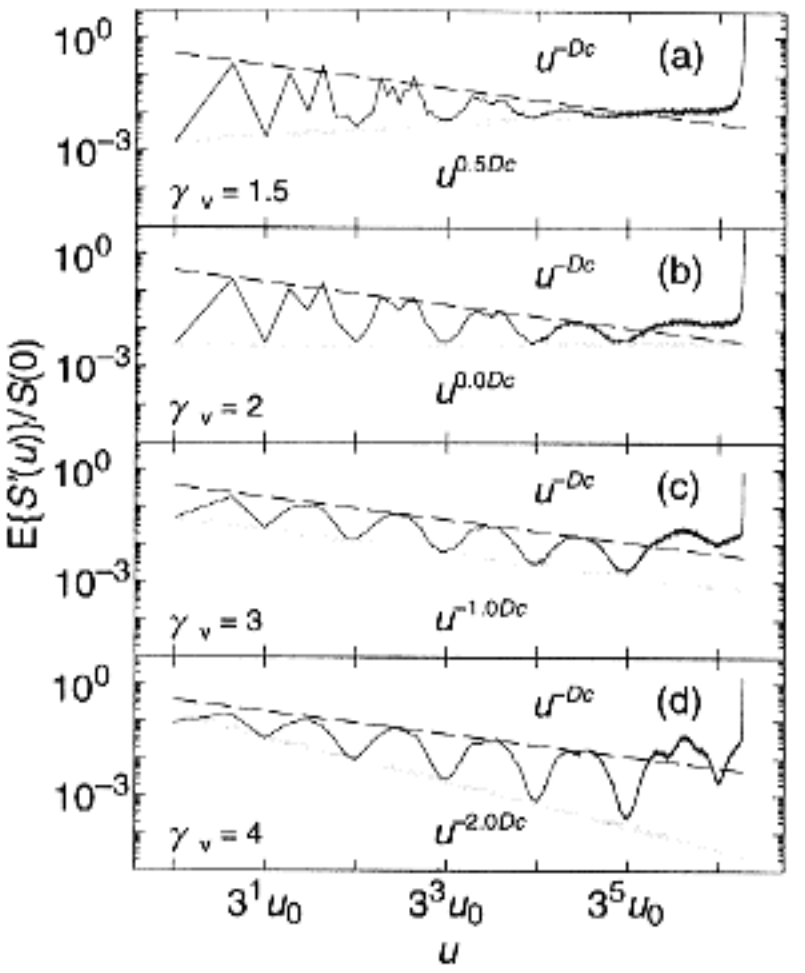

Fig. 3. Log–log representation of ensemble averages of modified power spectra of the modulated Cantor grating patterns calculated for surfaces with $\gamma_h = 3$, $N = 6$, and four different values of γ_v = (a)1.5, (b)2, (c)3, and (d)4 for the spatial frequency range of $(u_0, 3^6u_0)$, under the conditions of the incident angle $\theta_1 = 0°$ and the detecting angle $\theta_2 = 30°$. The results are normalized by the central peak value of a modified power spectrum for the regular Cantor grating pattern. The broken lines represent a power function u^{-D_c} and the gray lines represent power functions of (a)$u^{0.5D_c}$, (b)$u^{0.0D_c}$, (c)$u^{-1.0D_c}$, and (d)$u^{-2.0D_c}$.

where L is the whole width of the incident Cantor illumination.

Results of the present simulations show quite different features from those for the array illumination shown in Fig. 4(a)–(d). The simulation results in Fig. 4(a)–(d) is taken from Ref. [16]. When the scaling factor of the Cantor grating matches the horizontal scaling factor of the surface, namely, in the case of $\gamma_h = 3$, the calculated result shows very interesting features. Fig. 3(a)–(d) show the results for the self-affine surfaces with $\gamma_h = 3$, $N = 6$, and four different values of γ_v = (a)1.5, (b)2, (c)3, and (d)4, and with $\theta_1 = 0°$ and $\theta_2 = 30°$. It is seen in these figures that, in each case, the function $\mathrm{E}\{S'(u)\}/S(0)$ has maxima and minima periodically

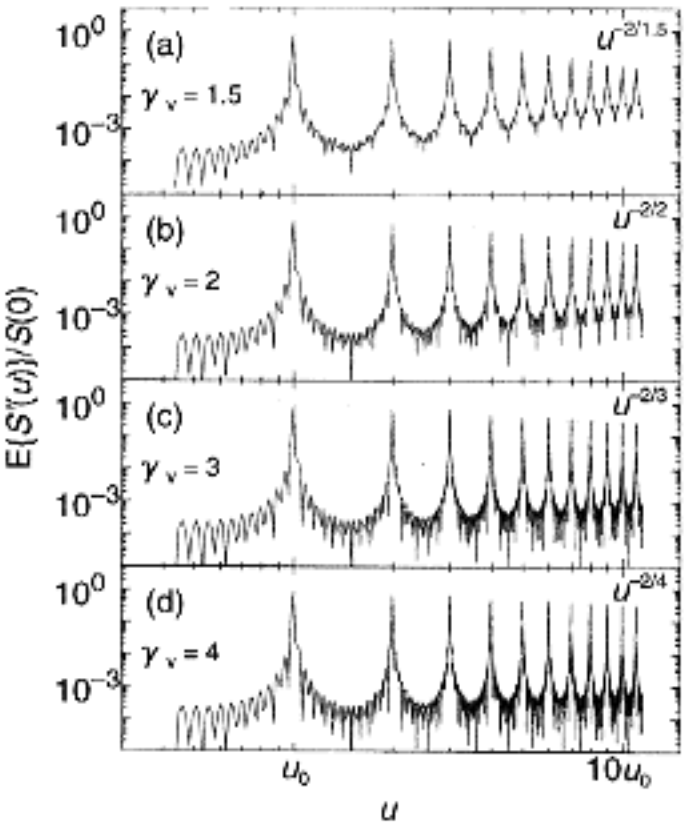

Fig. 4. Log–log representation of ensemble averages of modified power spectra of the modulated grating patterns evaluated for surfaces with $\gamma_h = 2$, $N = 6$, $\sigma_T = 0.1d$, and four different values of γ_v – (a)1.5, (b)2, (c)3, and (d)4 for the spatial frequency range of $(0.4u_0, 10u_0)$, under the conditions of $\theta_1 = 0°$ and $\theta_2 = 30°$. The results are normalized by the central peak value of a modified power spectrum for the regular grating. The gray lines represent the power functions of (a)$u^{-2/1.5}$, (b)$u^{-2/2}$, (c)$u^{-2/3}$, and (d)$u^{-2/4}$.

on the log scale, and that the logarithmical values of these maxima and minima depend linearly on $\log u$. The phenomenon of an abrupt raise of the curves in the region exceeding $3^6 u_0$, is due to a zero of $F(u)$, and is not an essential phenomenon, as mentioned in Refs. [16,17]. In these figures, the broken lines touching maxima of curves represent a power function u^{-D_c}. Here, D_c is the fractal dimension of the triadic Cantor grating and takes a value of log2/log3. On the other hand, the gray lines touching minima of curves represent power functions of (a)$u^{0.5D_c}$, (b)$u^{0.0D_c}$, (c)$u^{-1.0D_c}$, and (d)$u^{-2.0D_c}$, respectively. Therefore, it is clear that the minima obey the power law whose exponent depends upon the vertical scaling factor γ_v of the surface, while the maxima decrease with a power law u^{-D_c} in all cases. Furthermore, it is found from the numerical simulation that the exponent in the power law of minima takes a value of $(2 - \gamma_v)D_c$. It follows from this result that we can determine the value γ_v of scaling fluctuations in the self-affine surface from the observation of the minima of the function $E\{S'(u)\}/S(0)$.

A comparison between Fig. 3(a)–(d) and 4(a)–(d) indicates that a changing rate of the exponent $r = (2 - \gamma_v)D_c$ in the power law of minima for the Cantor illumination with an increase of the vertical scaling factor γ_v seems different from that of the exponent $r = -\gamma_h/\gamma_v$ in the power law of maxima for the array illumination. To make this point more clear, we calculate the absolute values $|\frac{\partial r}{\partial \gamma_v}|$ of partial differential coefficients of the exponent r with respect to the vertical scaling factor γ_v. Since the exponent r in the power law of the major maxima of the ensemble average of the modified power spectra produced by the array illumination is represented by $-\gamma_h/\gamma_v$ [16], its partial derivative is given by γ_h/γ_v^2. On the other hand, in case of $\gamma_h = 3$, the exponent r in the power law of the minima of the ensemble average of the modified power spectra produced by the Cantor illumination is represented by $(2 - \gamma_v)D_c$ and, hence, its partial derivative with respect to γ_v is given by $-D_c$. The above two derivatives with $\gamma_h = 3$ and $D_c = \log 2/\log 3$ are plotted in Fig. 5 as a function of γ_v for the range of (1.0, 5.0). From this figure, it is clear that the partial differential coefficient $|\frac{\partial r}{\partial \gamma_v}|$ corresponding to the array illumination decreases rapidly and nonlinearly with an increase of γ_v, while that corresponding to the Cantor illumination takes a constant value over the range. Therefore, the Cantor illumination provides a linear sensitivity with the

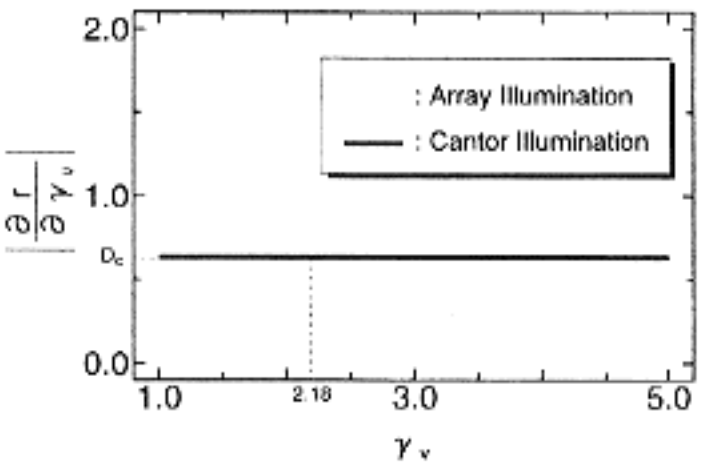

Fig. 5. Absolute values of partial differential coefficients of exponents in the two power laws: the power law of major maxima of the modified power spectra produced by the array illumination (gray curve), and the power law of minima of the modified power spectra produced by the Cantor illumination (black line). The horizontal scaling factor γ_h of the surface is set to 3.

value of γ_c, while the array illumination provides a nonlinear sensitivity.

In addition, the two partial differential coefficients are crossing at $\gamma_c = \sqrt{\gamma_h / D_c} \approx 2.18$. Therefore, in case of $2.18 < \gamma_c$, the method using the Cantor illumination is more sensitive than the method using the array illumination while, in case of $\gamma_c < 2.18$, the method using the array illumination becomes more sensitive than the other. It is noted that, in case of $\gamma_c < 1.00$, the surface model has a very unusual shape and cannot be effective as a model of practical surfaces. Hence, in most cases of γ_c, the Cantor illumination is advantageous over the array illumination. For the larger fractal dimension D_c, the Cantor illumination is advantageous in a wider range of γ_c. The Cantor illumination has another advantage. Since the minima of the partial differential coefficient in Fig. 3(a)–(d) are periodic in $\log u$, we can determine a decreasing ratio of the minima from the same number of data of the minima for different u's. In case of the array illumination, however, the interval of the major maxima of the coefficient is reduced with an increase of the spatial frequency [16], the number of data of the major maxima used to determine the decreasing ratio varies depending on the spatial frequency region.

This advantage of the Cantor illumination is a consequence of the scaling property of the illumination pattern which fits that of fluctuations in the surface. The Cantor grating is regarded as a multi-scale grating as shown in Fig. 2. Namely, the structure of each scale in the Cantor illumination can fit the fluctuations of the same scale on the rough surface, which causes a large variation of the power spectrum of the pattern. This advantage is also verified experimentally in the next section.

4. Experiment

The experimental setup is represented in Fig. 6 which is the same with that used in the array illumination experiment, apart from the incident light pattern [16]. The Cantor illumination is effectively realized by the scanning method. A spot is formed on a surface by a Gaussian beam from a He-Ne laser which is incident normally upon the surface. An image of the spot is detected by a CCD camera with the detecting angle of $\theta_2 = 30°$ and is fed into a computer through a frame memory. The horizontal position of this spot image in the CCD plane is shifted due to the height of surface as shown in Fig. 1(b), and hence the shifted spot image includes the information about the height of the object surface at the illuminating point. In the same way, the next spot image is recorded on the frame memory, after a suitable lateral shift of the object. When the whole surface has been scanned in this way, the recorded spot images are superposed in a computer to give the modulated grating pattern.

As fractal surfaces, three different rumpled sheet materials, which were used in Ref. [16], were also employed as fractal surfaces: rumpled 15 μm thick aluminum foil which is known to form a fractal surface with a multi-scale rough shape [11,18], rumpled thin paper for a copy machine, and rumpled vinyl-coated paper. The RMS-roughness was measured in a square area of $150 \times 150\text{mm}^2$ for these materials and found to be 5.9mm, 4.7mm, and

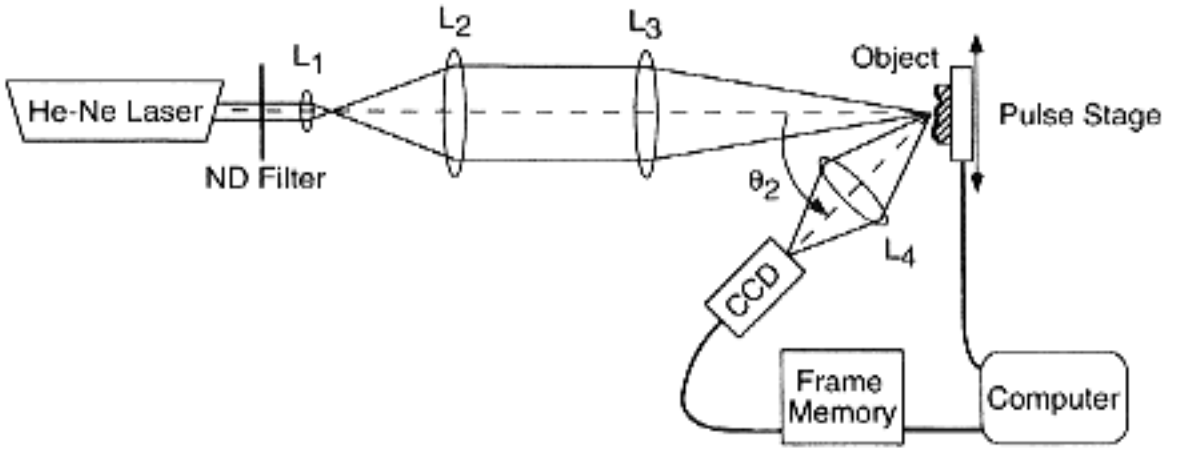

Fig. 6. Experimental setup.

5.7mm, respectively. Since the surfaces include fluctuations with a wide range of amplitude to realize the scaling property of a large level, these RMS-roughnesses take somewhat large values. By using this experimental system and these surface materials, a set of data having 50 data of modulated Cantor patterns produced experimentally on a surface is provided for each surface. In each case, from these data, the ensemble-average $E\{S'(u)\}$ of the modified power spectra of modulated Cantor patterns is calculated and, then, the results normalized by the central peak value $S(0)$ of a modified power spectrum for the Cantor pattern without fluctuations are shown logarithmically in Fig. 7(a)–(c) as a function of the spatial frequency u for $(u_0, 3^6 u_0)$. Here, the spatial frequency u_0 is calculated from Eq. (5) and takes a value of $7.8\mathrm{m}^{-1}$, under the conditions of the incident angle $\theta_1 = 0°$ and the detecting angle $\theta_2 = 30°$. The results in Fig. 7(a)–(c) are corresponding to the rough surfaces made of the aluminum foil, thin paper, and vinyl-coated paper, respectively.

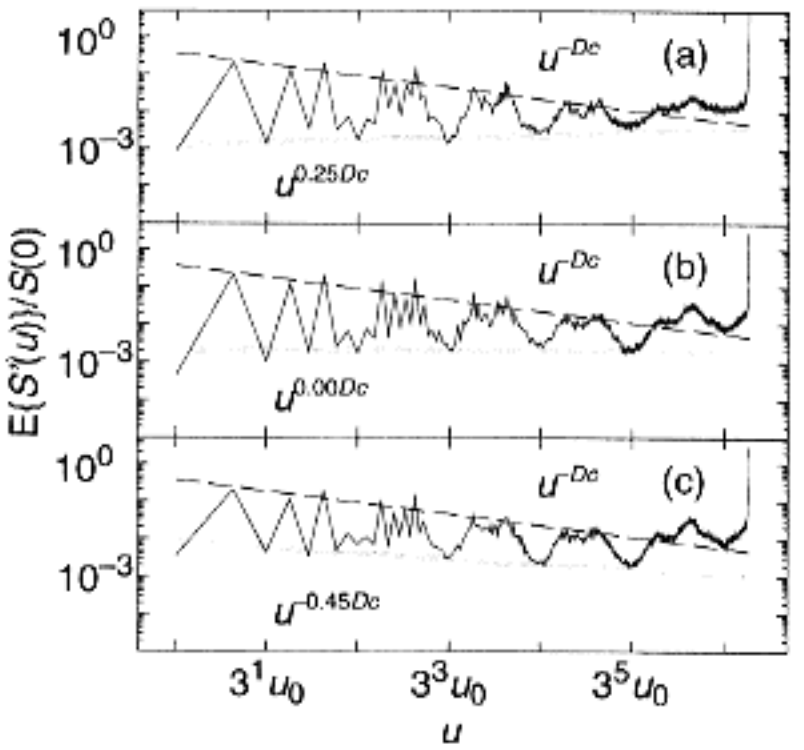

Fig. 7. Log–log representation of ensemble averages of the modified power spectra of modulated Cantor grating patterns produced experimentally on rumpled surfaces made of (a) 15-μm-thick aluminum foil, (b) thin paper, and (c) vinyl-coated paper for the spatial frequency range of $(u_0, 3^6 u_0)$, under the condition of the incident angle $\theta_1 = 0°$ and the detecting angle $\theta_2 = 30°$. The results are normalized by the central peak value of a modified power spectrum for the regular Cantor grating pattern. The broken lines represent a power function u^{-D_c} and the gray lines represent power functions of (a)$u^{0.25D_c}$, (b)$u^{0.00D_c}$, and (c)$u^{-0.45D_c}$.

From these figures, it is recognized that, in each case, the coefficient $E\{S'(u)\}/S(0)$ has maxima and minima periodically on the log scale and that the logarithmical values of maxima and minima decrease linearly with $\log u$. In these figures, the broken lines touching maxima of curves represent a power functions u^{-D_c}, where D_c is the fractal dimension of the triadic Cantor grating and takes a value of log2/log3, while the gray lines touching minima of curves represent power functions of $u^{0.25D_c}$, $u^{0.00D_c}$, and $u^{-0.45D_c}$, respectively. It is noted that, in each case, the height of minima varies with the power law whose exponent is changed by the surface, while the height of maxima decreases with the power law u^{-D_c} in every case. Therefore, it is clear that these results are congruous with those of simulations representing Fig. 3(a)–(d). Accordingly, we can determine the vertical scaling factor γ_v of rough surfaces from these results and the relation revealed by simulations in the previous section. As a result, the evaluated values of γ_v for three object surfaces of aluminum foil, thin paper, and vinyl-coated paper are approximately 1.75, 2.00, and 2.45, respectively. These values agree with those evaluated by the method using the array illumination in Ref. [16]. Furthermore, it is recognized that a changing quantity of the exponent in the power law of this method with an increase of the vertical scaling factor γ_v of the surface is bigger than that in the method using the array illumination shown in Ref. [16].

Consequently, it is clear that the method using the Cantor illumination is more advantageous than the method using the array illumination for an evaluation of the scaling property of fractal surfaces, apart from the case that the vertical scaling factor γ_v of the surface has the value close to 1.0 and that very sensitive measurements of γ_v are needed.

5. Conclusion

To evaluate the scaling property of fractal surfaces, an optical method using the Cantor illumination was introduced. It was applied to several fractal surfaces and the property of this method was investigated by means of computer simulations. The results were compared with those for the method using the array illumination.

In simulations, self-affine surfaces with various values of parameters were employed as fractal surface models. The ensemble average of the modified power spectra of the Cantor grating patterns, which are randomized by fractal surfaces, was calculated numerically. From the simulations, it was elucidated that these ensemble-averaged spectra have maxima and minima periodically on the log scale, and that the logarithmical values of these extrema vary linearly with $\log u$. The height of minima varies with the power law $u^{(2-\gamma_v)D_c}$, while the height of maxima decreases with the power law u^{-D_c}, where D_c is a fractal dimension of the triadic Cantor grating and takes a value of log2/log3. This result allows us to determine values of the scaling factor γ_v of self-affine surfaces.

To compare the sensitivity of the slope to a change of the scaling factor, absolute values of partial differential coefficients of the exponents in the power laws for the two illumination methods were calculated. It was made clear that the coefficient for the array illumination decreases rapidly and nonlinearly with an increase of γ_v, while the coefficient for the Cantor illumination is constant. The array and Cantor illuminations show nonlinear and linear sensitivities, respectively. Therefore, a higher sensitivity is provided by the array illumination for $\gamma_v < \sqrt{\gamma_h/D_c}$, and by the Cantor illumination for $\sqrt{\gamma_h/D_c} < \gamma_v$. In addition, the number of major maxima and minima used to determine the power law is constant for the Cantor illumination, but it is not constant for the array illumination and varies depending on the spatial frequency region. From these results, the Cantor illumination is more advantageous than the array illumination to evaluate the fractality of rough surfaces.

The results of simulations are verified by the experiment. Three different rumpled sheet materials having the scaling property were tested. In each case, the coefficient has maxima and minima periodically on the log scale, and that the values of minima vary with the power law depending upon the scaling property of the object surface, while the values of minima decrease with a power law which is independent of the scaling property of the surface. These results agree with those of simulations. In addition, the evaluated scaling factors well described the feature of each random surface.

In this paper, the one-dimensional Cantor illumination was introduced. Although such an illumination is enough to analyze isotropic two-dimensional (2D) surfaces as the case of the present experiment, this method can be extended easily, if necessary, to anisotropic 2D fractal surfaces by introducing a 2D fractal illumination, e.g. a Cantor mesh or a 2D scanning method.

Finally, the proposed method will be useful for analyzing conditions of actual surfaces having fractality, such as natural surfaces of rock and soil, rumpled surfaces of paper and thin films, and surfaces of various materials processed mechanically or chemically.

Appendix A

The self-affine surfaces employed in the present simulation are produced by superposing many random processes which have different standard devia-

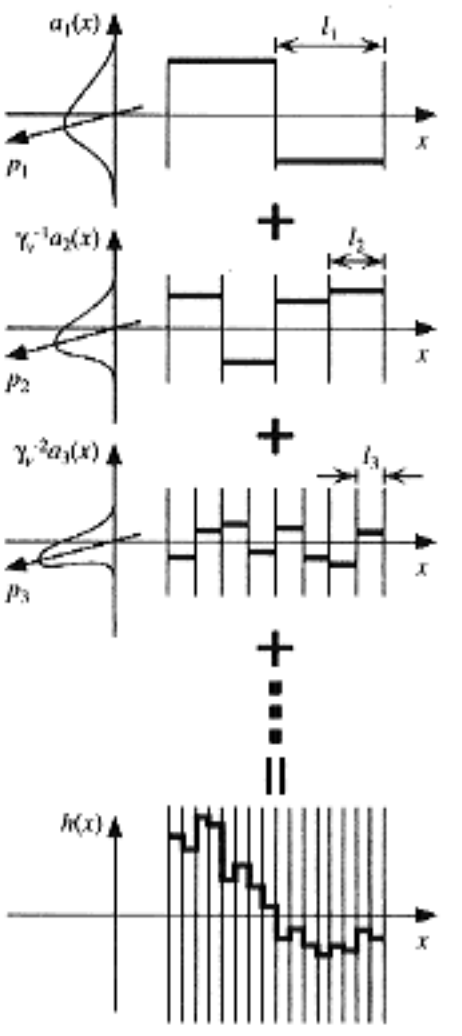

Fig. 8. Schematic representation of the generating procedure of self-affine surfaces.

tions and correlation lengths as shown in Fig. 8. In Eq. (2), γ_v is a vertical scaling factor controlling the relative standard deviation of each random process and, hence, governs the vertical scaling property of the surface. On the other hand, γ_h in Eq. (3) is a factor determining the relative correlation length of each random process and governing the horizontal scaling property and is called a horizontal scaling factor. As a combination of these two scaling properties, these factors determine the fractality of the surface. Namely, respective magnification in the vertical and horizontal directions with the factors of γ_v and γ_h yields the same structure as the original in a statistical sense, which is the self-affinity.

References

[1] B.B. Mandelbrot, The Fractal Geometry of Nature, Freeman, New York, 1982.
[2] J. Feder, Fractals, Plenum, New York, 1988.
[3] M. Barnsley, Fractals Everywhere, Academic Press, San Diego, 1988.
[4] H.-O. Peitgen, D. Saupe (Eds.), The Science of Fractals Images, Springer-Verlag, New York, 1988.
[5] T. Vicsek, Fractal Growth Phenomena, World Scientific, Singapore, 1989.
[6] A. Aharony, J. Feder, (Eds.), Fractals in Physics, North-Holland, Amsterdam, 1990, (reprinted from Physica D, vol. 38, Nos. 1–3, 1989).
[7] E. Jakeman, J. Phys. A: Math. Gen. 15 (1982) L55.
[8] M.V. Berry, J. Phys. A: Math. Gen. 12 (1979) 781.
[9] D.L. Jaggard, X. Sun, J. Opt. Soc. Am. A 7 (1990) 1131.
[10] P. Wong, A.J. Bray, Phys. Rev. B 37 (1988) 7751.
[11] D.L. Jordan, F. Moreno, Waves Random Media 2 (1992) 29.
[12] A. Dogariu, J. Uozumi, T. Asakura, Pure Appl. Opt. 2 (1993) 339.
[13] B.L. Cox, J.S.Y. Wang, Fractals 1 (1993) 87.
[14] S. Frankenthal, A.M. Whitman, J. Opt. Soc. Am. A 6 (1989) 1827.
[15] S.K. Sinha, E.B. Sirota, S. Garoff, H.B. Stanley, Phys. Rev. B 38 (1988) 2297.
[16] N. Wada, J. Uozumi, T. Asakura, Opt. Commun. 134 (1997) 264.
[17] N. Wada, J. Uozumi, T. Asakura, Opt. Commun. 130 (1996) 122.
[18] D.L. Jordan, F. Moreno, J. Opt. Soc. Am. A 10 (1993) 1989.